Diffusion generated methods for target-valued maps

Braxton Osting

University of Utah

July, 2018

BIRS workshop on Spectral Geometry

Based on joint work with Dong Wang and Ryan Viertel

Mean curvature flow

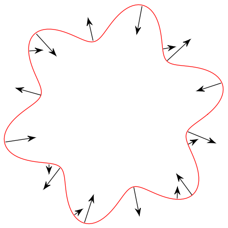

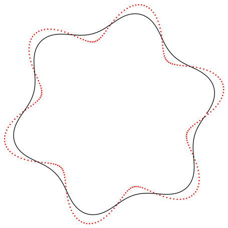

Mean curvature flow arises in a variety of physical applications

- Related to surface tension
- A model for the formation of grain boundaries in crystal growth

Some ideas for numerical computation:

- we could parameterize the surface and compute

$$H = -\frac{1}{2}\nabla \cdot \hat{n}$$

- If the surface is implicitly defined by the equation $F(x, y, z) = 0$, then mean curvature can be computed

$$H = -\frac{1}{2}\nabla \cdot \left(\frac{\nabla F}{|\nabla F|} \right)$$

MBO diffusion generated method

In 1992, Merriman, Bence, and Osher (MBO) developed an iterative method for evolving an interface by mean curvature.

Repeat:

Step 1. Solve the Cauchy problem for the diffusion equation (heat equation)

$$u_t = \Delta u$$
$$u(x, t = 0) = \chi_D,$$

with initial condition given by the indicator function χ_D of a domain D until time τ to obtain the solution $u(x, \tau)$.

Step 2. Obtain a domain D_{new} by thresholding:

$$D_{\text{new}} = \left\{ x \in \mathbb{R}^d : u(x, \tau) \geq \frac{1}{2} \right\}.$$

How to understand the MBO diffusion generated method?

From pictures, one can easily see:

- diffusion quickly blunts sharp points on the boundary and
- diffusion has little effect on the flatter parts of the boundary.

Formally, consider a point $P \in \partial D$. In local polar coordinates with the origin at P, the diffusion equation is given by

$$\frac{\partial u}{\partial t} = \frac{1}{r}\frac{\partial u}{\partial r} + \frac{\partial^2 u}{\partial r^2} + \frac{1}{r^2}\frac{\partial^2 u}{\partial \theta^2}.$$

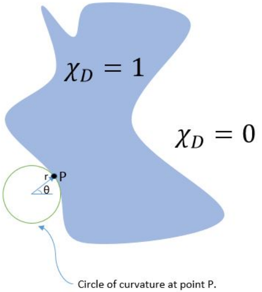

Considering local symmetry, we have

$$\begin{aligned}\frac{\partial u}{\partial t} &= \frac{1}{r}\frac{\partial u}{\partial r} + \frac{\partial^2 u}{\partial r^2} \\ &= {\color{red}H}\frac{\partial u}{\partial r} + \frac{\partial^2 u}{\partial r^2}.\end{aligned}$$

The $\frac{1}{2}$ level set will move in the normal direction with velocity given by the mean curvature, H.

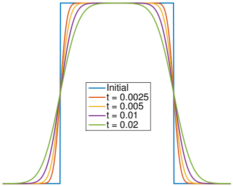

A variational point of view: Modica+Mortola, Allen+Cahn, Ginzburg+Landau

Define the energy

$$J_\varepsilon(u) = \int_\Omega \frac{1}{2}|\nabla u(x)|^2 + \frac{1}{\varepsilon^2} W(u(x))\, dx$$

where $W(u) = \frac{1}{4}\left(u^2 - 1\right)^2$ is a double well potential.

Theorem (Modica+ Mortola, 1977) A minimizing sequence (u_ε) converges (along a subsequence) to $\chi_D - \chi_{\Omega\setminus D}$ in L^1 for some $D \subset \Omega$. Furthermore,

$$\varepsilon J_\varepsilon(u_\varepsilon) \to \frac{2\sqrt{2}}{3}\mathcal{H}^{d-1}(\partial D) \qquad \text{as } \varepsilon \to 0.$$

Gradient flow. The L^2 gradient flow of J_ε gives the Allen-Cahn equation:

$$u_t = \Delta u - \frac{1}{\varepsilon^2} W'(u) \qquad \text{in } \Omega.$$

Operator/energy splitting. Repeat the following two steps:

- **Step 1.** Solve the diffusion equation until time τ with initial condition $u(x, t = 0) = \chi_D$

$$\partial_t u = \Delta u$$

- **Step 2.** Solve the (pointwise defined!) equation until time τ:

$$\phi_t = -W'(\phi)/\varepsilon^2, \quad \phi(x, 0) = u(x, \tau), \qquad \text{in } \Omega.$$

- **Step 2*.** Rescaling $\tilde{t} = \varepsilon^{-2} t$, we have as $\varepsilon \to 0$, $\varepsilon^{-2}\tau \to \infty$. So, Step 2 is equivalent to thresholding:

$$\phi(x, \infty) = \begin{cases} 1 & \text{if } \phi(x, 0) > 1/2 \\ 0 & \text{if } \phi(x, 0) < 1/2 \end{cases}.$$

Analysis, extensions, applications, connections, and computation

- Proof of convergence of the MBO method to mean curvature flow [Evans1993, Barles and Georgelin 1995, Chambolle and Novaga 2006, Laux and Swartz 2017, Swartz and Yip 2017].

- Multi-phase problems with arbitrary surface tensions [Esedoglu and Otto 2015, Laux and Otto 2016]

- Numerical algorithms [Ruuth 1996, Ruuth 1998]
- Adaptive methods based on NUFFT [Jiang et. al. 2017]

- Micromagnetics [Wang et. al. 2001]
- Volume preserving interface motion [Ruuth 2003] auction dynamics [Jacobs et. al. 2017]
- Image processing [Esedoglu et al. 2006, Merkurjev et al. 2013, Wang et. al. 2017]
- Problems of anisotropic interface motion [Merriman et al. 2000, Ruuth et al. 2001, Bonnetier et al. 2010, Elsey et al. 2016]
- Diffusion generated method using signed distance function [Esedoglu et al. 2009]
- High order geometric flows [Esedoglu 2008]
- Nonlocal threshold dynamics method [Caffarelli and Souganidis 2010]
- Wetting problem on solid surfaces [Xu et. al. 2017],
- Graph partitioning and data clustering [van Gennip et. al. 2013]
- Centroidal Voronoi Tessellation [Du 1999]

Target-valued maps

Let $\Omega \subset \mathbb{R}^d$ be a bounded domain with smooth boundary.
Let $T \subset \mathbb{R}^k$ be the "target set".
We consider maps $u\colon \Omega \to T$.

Examples:

- $\mathbb{S}^1$
- $\mathbb{RP}^1$
- $\mathrm{SPD}(3)$
- Σ_5

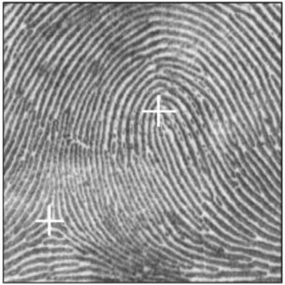

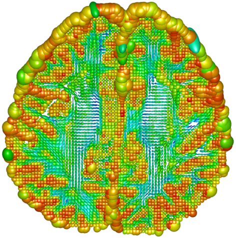

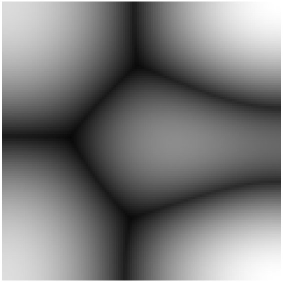

Harmonic target-valued maps

Let $\Omega \subset \mathbb{R}^d$ be a bounded domain with smooth boundary.
Let $T \subset \mathbb{R}^k$ be the "target set".

Consider the general variational problem,

$$\inf_{u\colon \Omega \to T} E(u) \qquad \text{where} \quad E(u) = \frac{1}{2}\int_\Omega |\nabla u|^2 \, dx$$

Energy relaxation via penalization.
Let $L\colon \mathbb{R}^k \to \mathbb{R}_+$ be a smooth function such that $T = L^{-1}(0)$.
$\implies$ T is the set of global minimizers of the non-negative function L.
Roughly, we want $L(x) \approx \text{dist}^2(x, T)$.

Relax the energy to obtain:

$$\min_{u \in H^1(\Omega;\mathbb{R}^k)} E_\varepsilon(u) \qquad \text{where} \quad E_\varepsilon(u) = \frac{1}{2}\int_\Omega |\nabla u|^2 \, dx + \frac{1}{\varepsilon^2}\int_\Omega L\left(u(x)\right) \, dx.$$

Examples.

k	T	L(x)	comment
1	$\{\pm 1\}$	$\frac{1}{4}(x^2-1)^2$	Allen-Cahn
2	$\mathbb{S}^1$	$\frac{1}{4}(\lvert x\rvert^2-1)^2$	Ginzburg-Landau
n^2	$O(n)$	$\frac{1}{4}\lVert x^t x - I_n\rVert_F^2$	orthogonal matrix-valued field
k	convex set $T \subset R^k$	$\frac{1}{2}d^2(x,T)$	
k	coordinate axes, Σ_k	$\frac{1}{4}\sum_{i\neq j} x_i^2 x_j^2$	Dirichlet partitions
	$\mathbb{RP}^1$		line field

A diffusion generated method for the Ginzburg-Landau model

$$E_\varepsilon(u) = \int_\Omega \frac{1}{2}|\nabla u(x)|^2 \; + \; \frac{1}{4\varepsilon^2}\left(|u(x)|^2 - 1\right)^2 \; dx.$$

k	T	L(x)	comment
2	$\mathbb{S}^1$	$\frac{1}{4}(\lvert x\rvert^2 - 1)^2$	Ginzburg-Landau

The closest-point map, $\Pi_T : \mathbb{R}^2 \to T$, for $T = \mathbb{S}^1$ is given by

$$\Pi_T x = \frac{x}{|x|}.$$

- S. J. Ruuth, B. Merriman, J. Xin, and S. Osher, Diffusion-Generated Motion by Mean Curvature for Filaments, J. Nonlinear Sci. **11** (2001).

Diffusion generated method. For $i = 1, 2, \ldots$,

- **Step 1.** Solve the diffusion equation until time τ

$$\partial_t u = \Delta u$$
$$u(x, t = 0) = \phi_i$$

- **Step 2.** Point-wise, apply the closest-point map:

$$\phi_{i+1}(x) = \Pi_T u(x, \tau).$$

Application: Quad meshing
— joint work with Ryan Viertel (U. Utah)

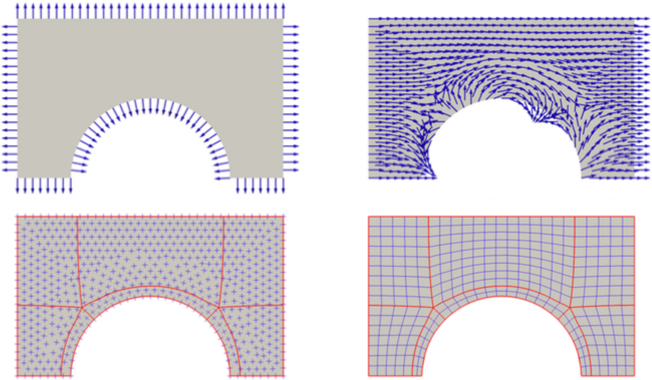

FIG. 2. **Overview of the cross field based meshing methods.** **(top left)** *The domain is shown with outward pointing normals.* **(top right)** *A 4-aligned boundary condition is assigned (see* Definition 3.12*) and a representation vector field is found by approximately minimizing the Ginzburg-Landau energy.* **(bottom left)** *The representation field is mapped to a smooth cross field and separatrices of the cross field are traced to partition the domain into a quad layout.* **(bottom right)** *A regular mesh is mapped into each region.*

Theorem [Viertel + O. (2017)] If no separatrix of u converges to a limit cycle, then the separatrices of U, along with ∂D partition D into a 4 sided partition.

Examples of quad meshes

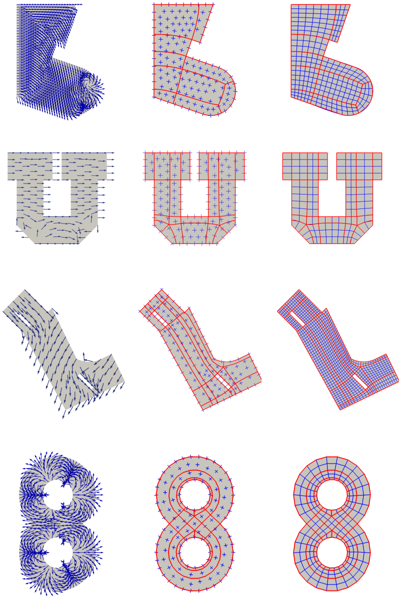

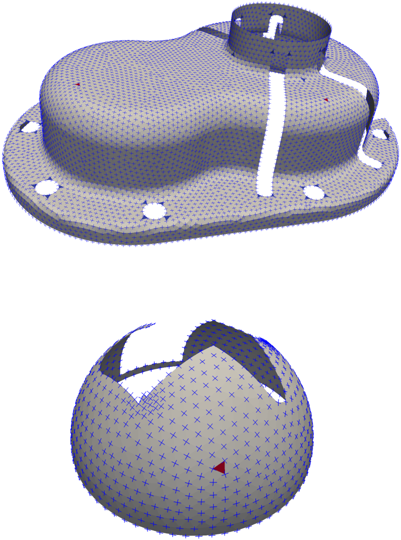

Orthogonal matrix valued fields — joint work with Dong Wang (U. Utah)

Let $O_n \subset M_n = \mathbb{R}^{n\times n}$ be the group of orthogonal matrices.

$$\inf_{A:\ \Omega\to O_n} E(A), \qquad \text{where } E(A) := \frac{1}{2}\int_\Omega \|\nabla A\|_F^2 \, dx.$$

Relaxation:

$$\min_{A\in H^1(\Omega;M_n)} E_\varepsilon(A), \qquad \text{where } E_\varepsilon(A) := E(A) + \frac{1}{4\varepsilon^2}\int_\Omega \|A^tA - I_n\|_F^2 \, dx.$$

The penalty term can be written:

$$\frac{1}{4\varepsilon^2}\|A^tA - I_n\|_F^2 = \frac{1}{\varepsilon^2}\sum_{i=1}^n W(\sigma_i(A)), \qquad \text{where } W(x) = \frac{1}{4}\left(x^2-1\right)^2.$$

Gradient Flow. The gradient flow of E_ε is

$$\partial_t A = -\nabla_A E_\varepsilon(A) = \Delta A - \varepsilon^{-2}A(A^tA - I_n).$$

Special cases.

- For $n = 1$, we recover Allen-Cahn equation.
- For $n = 2$, if the initial condition is taken to be in $SO(2) \cong S^1$, we recover the complex Ginzburg-Landau equation.

Diffusion generated method for O_n valued fields

$$E_\varepsilon(A) := \int_\Omega \frac{1}{2}\|\nabla A\|_F^2 + \frac{1}{4\varepsilon^2}\|A^tA - I_n\|_F^2 \, dx.$$

k	T	L(x)	comment
n^2	$O(n)$	$\frac{1}{4}\|x^tx - I_n\|_F^2$	orthogonal matrix valued fields

Lemma. The closest-point map, $\Pi_T : \mathbb{R}^{n\times n} \to T$, for $T = O_n$ is given by

$$\Pi_T A = A(A^tA)^{-\frac{1}{2}} = UV^t,$$

where A has the singular value decomposition, $A = U\Sigma V^t$.

Diffusion generated method. For $i = 1, 2, \ldots$,

- **Step 1.** Solve the diffusion equation until time τ

$$\partial_t u = \Delta u$$
$$u(x, t = 0) = \phi_i$$

- **Step 2.** Point-wise, apply the closest-point map:

$$\phi_{i+1}(x) = \Pi_T u(x, \tau).$$

Lyapunov function for MBO iterates

Let Ω be a closed surface.
Motivated by (Esedoglu + Otto, 2015), we define the functional $E^\tau : L^2(\Omega; M_n) \to \mathbb{R}$, given by

$$E^\tau(A) := \frac{1}{\tau} \int_\Omega n - \langle A, e^{\Delta\tau} A\rangle_F \, dx$$

Here, $e^{\tau\Delta}A$ denotes the solution to the diffusion equation at time τ with initial condition at time $t = 0$ given by $A = A(x)$.

Denoting the spectral norm by $\|A\|_2 = \sigma_{\max}(A)$, the convex hull of O_n is

$$K_n = \text{conv } O_n = \{A \in M_n \colon \|A\|_2 \le 1\}.$$

Lemma. The functional E^τ has the following elementary properties.

(i) For $A \in L^2(\Omega; O_n)$, $\quad E^\tau(A) = E(A) + O(\tau)$.

(ii) $E^\tau(A)$ is concave.

(iii) We have

$$\min_{A \in L^2(\Omega; O_n)} E^\tau(A) = \min_{A \in L^2(\Omega; K_n)} E^\tau(A).$$

(iv) $E^\tau(A)$ is Fréchet differentiable with derivative $L^\tau_A : L^\infty(\Omega; M_n) \to \mathbb{R}$ at A in the direction B given by

$$L^\tau_A(B) = -\frac{2}{\tau} \int_\Omega \langle e^{\Delta\tau} A, B\rangle_F \, dx.$$

Stability

The *sequential linear programming* approach to minimizing $E^\tau(A)$ subject to $A \in L^\infty(\Omega; K_n)$ is to consider a sequence of functions $\{A_s\}_{s=0}^\infty$ which satisfies

$$A_{s+1} = \arg \min_{A \in L^\infty(\Omega; K_n)} L^\tau_{A_s}(A), \qquad A_0 \in L^\infty(\Omega; O_n) \text{ given.}$$

Lemma. If $e^{\Delta\tau} A_s = U \Sigma V^t$, the solution to the linear optimization problem,

$$\min_{A \in L^\infty(\Omega; K_n)} L^\tau_{A_s}(A).$$

is attained by the function $A^\star = UV^t \in L^\infty(\Omega; O_n)$.

Thus, $A_s \in L^\infty(\Omega; O_n)$ for all $s \geq 0$ and these are precisely the iterations in the generalized MBO diffusion generated method!

Theorem (Stability). [O. + Wang, 2017] The functional E^τ is non-increasing on the iterates $\{A_s\}_{s=1}^\infty$, *i.e.*, $E^\tau(A_{s+1}) \leq E^\tau(A_s)$.

Proof. By the concavity of E^τ and linearity of $L^\tau_{A_s}$,

$$E^\tau(A_{s+1}) - E^\tau(A_s) \leq L^\tau_{A_s}(A_{s+1} - A_s) = L^\tau_{A_s}(A_{s+1}) - L^\tau_{A_s}(A_s).$$

Since $A_s \in L^\infty(\Omega; K_n)$, $L^\tau_{A_s}(A_{s+1}) \leq L^\tau_{A_s}(A_s)$ which implies $E^\tau(A_{s+1}) \leq E^\tau(A_s)$. $\square$

Convergence

We consider a discrete grid $\tilde{\Omega} = \{x_i\}_{i=1}^{|\tilde{\Omega}|} \subset \Omega$ and a standard finite difference approximation of the Laplacian, $\tilde{\Delta}$, on $\tilde{\Omega}$. For $A \colon \tilde{\Omega} \to O_n$, define the discrete functional

$$\tilde{E}^{\tau}(A) = \frac{1}{\tau} \sum_{x_i \in \tilde{\Omega}} 1 - \langle A_i, (e^{\tilde{\Delta}\tau} A)_i \rangle_F$$

and its linearization by

$$\tilde{L}_A^{\tau}(B) = -\frac{2}{\tau} \sum_{x_i \in \tilde{\Omega}} \langle B_i, (e^{\tilde{\Delta}\tau} A)_i \rangle_F.$$

Theorem (Convergence for $n = 1$.) [O. + Wang, 2017]
Let $n = 1$. Non-stationary iterations of the generalized MBO diffusion generated method strictly decrease the value of $\tilde{E}^{\tau}$ and since the state space is finite, $\{\pm 1\}^{|\tilde{\Omega}|}$, the algorithm converges in a finite number of iterations. Furthermore, for $m := e^{-\|\tilde{\Delta}\|\tau}$, each iteration reduces the value of J by at least $2m$, so the total number of iterations is less than $\tilde{E}^{\tau}(A_0)/2m$.

Theorem (Convergence for $n \geq 2$.) [O. + Wang, 2017]
Let $n \geq 2$. The non-stationary iterations of the generalized MBO diffusion generated method strictly decrease the value of $\tilde{E}^{\tau}$. For a given initial condition $A_0 \colon \tilde{\Omega} \to O_n$, there exists a partition $\tilde{\Omega} = \tilde{\Omega}_+ \amalg \tilde{\Omega}_-$ and an $S \in \mathbb{N}$ such that for $s \geq S$,

$$\det A_s(x_i) = \begin{cases} +1 & x_i \in \tilde{\Omega}_+ \\ -1 & x_i \in \tilde{\Omega}_- \end{cases}.$$

Lemma. $\operatorname{dist}\big(SO(n),\ SO^-(n)\big) = 2.$

Dirichlet partitions

A collection of k disjoint open sets, $U_1, \ldots, U_k \subseteq \Omega$ is a *Dirichlet k-partition of* Ω if it attains

$$\inf_{\substack{U_\ell \subset \Omega \\ U_\ell \cap U_m = \emptyset}} \sum_{\ell=1}^{k} \lambda_1(U_\ell) \qquad \text{where} \quad \lambda_1(U) := \min_{\substack{u \in H_0^1(\Omega) \\ \|u\|_{L^2(\Omega)}=1}} E(u).$$

$\Longrightarrow$ $\lambda_1(\Omega)$ is the first Dirichlet e.val. of $-\Delta$ on Ω.

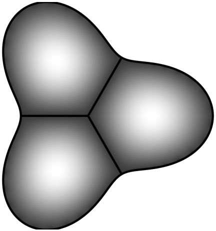

3-partition of $\Omega \subset \mathbb{R}^2$

Mapping formulation

Consider the target set given by the coordinate axes,

$$T = \Sigma_k := \left\{ x \in \mathbb{R}^k \colon \sum_{i \neq j}^{k} x_i^2 x_j^2 = 0 \right\}.$$

The Dirichlet partition problem for Ω is equivalent to the mapping problem

$$\min \left\{ E(u) \colon u \in H_0^1(\Omega; \Sigma_k), \int_\Omega u_\ell^2(x)\, dx = 1 \text{ for all } \ell \in [k] \right\},$$

where E is the Dirichlet energy and $H_0^1(\Omega; \Sigma_k) = \{ u \in H_0^1(\Omega; \mathbb{R}^k) \colon u(x) \in \Sigma_k \text{ a.e.} \}$.

We refer to minimizers u as *ground states* and WLOG take $u \geq 0$ and quasi-continuous.

$$u \text{ is a ground state}$$
$$\Longleftrightarrow$$
$$\Omega = \amalg_\ell U_\ell \text{ with } U_\ell = u_\ell^{-1}\big((0,\infty)\big) \text{ for } \ell \in [k] \text{ is a Dirichlet partition.}$$

Cafferelli and Lin (2007) used reformulation to prove regularity results, such as $C^{1,\alpha}$-smoothness of the partition interfaces away from a set of codimension two.

Diffusion generated method for computing Dirichlet partitions — joint work with Dong Wang (U. Utah)

k	T	L(x)	comment
k	coordinate axes, Σ_k	$\frac{1}{4}\sum_{i\neq j} x_i^2 x_j^2$	Dirichlet partitions

Relaxed energy: $E_\varepsilon(u) = \frac{1}{2}\int_\Omega |\nabla u|^2 \, dx \; + \; \frac{1}{4\varepsilon^2}\int_\Omega \sum_{i\neq j} u_i^2(x) u_j^2(x)\, dx$
Relaxed problem:

$$\min_{u\in H^1(\Omega;\mathbb{R}^k)} E_\varepsilon(u)$$
$$\text{s.t. } \|u_j\|_{L^2(\Omega)} = 1$$

The closest-point map, $\Pi_T : \mathbb{R}^k \to T$, for $T = \Sigma_k$ is given by

$$(\Pi_T x)_i = \begin{cases} x_i & x_i = \max_j x_j \\ 0 & \text{otherwise} \end{cases}.$$

Diffusion generated method. For $i = 1, 2, \ldots,$

- **Step 1.** Solve the diffusion equation until time τ

$$\partial_t u = \Delta u$$
$$u(x, t = 0) = \phi_i$$

- **Step 2.** Point-wise, apply the closest-point map:

$$\tilde{\phi}(x) = \Pi_T u(x,\tau).$$

- **Step 3.** Normalize:

$$\phi_{i+1}(x) = \frac{\tilde{\phi}(x)}{\|\tilde{\phi}\|_{L^2(\Omega)}}.$$

Results for 2D flat tori, $k = 3$–$9,11,12,15,16$, and 20

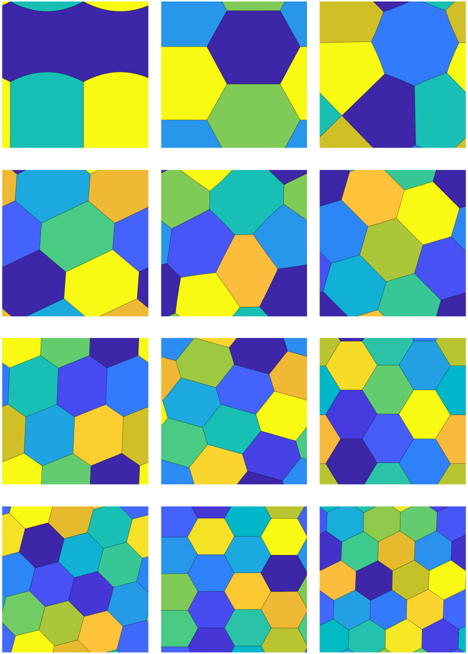

Results for 3D flat tori, $k = 2$

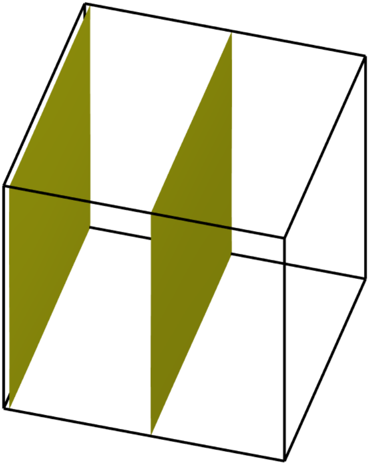

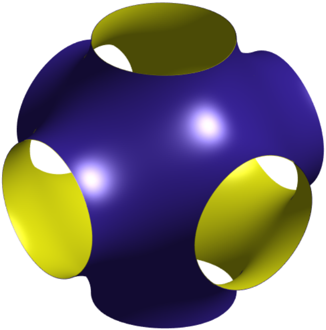

Results for 3D flat tori, $k = 4$, tessellation by rhombic dodecahedra

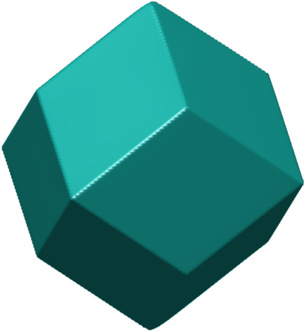

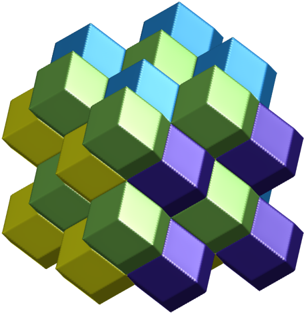

Results for 3D flat tori, $k = 12$, Kelvin's structure composed of truncated octahedra

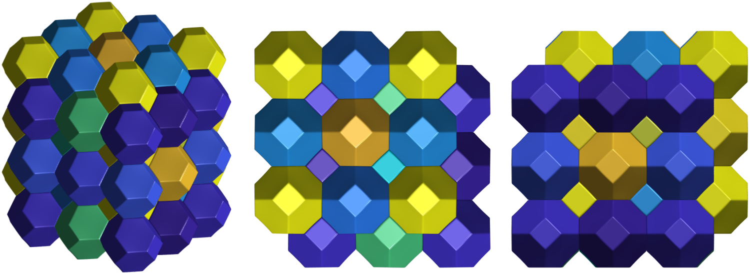

Results for 3D flat tori, $k = 8$, Weaire-Phelan structure

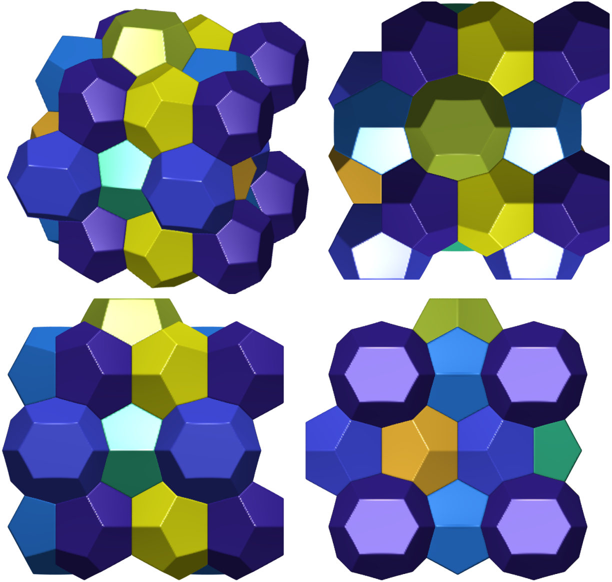

Results for 4D flat tori, $k = 8$, 24-cell honeycomb

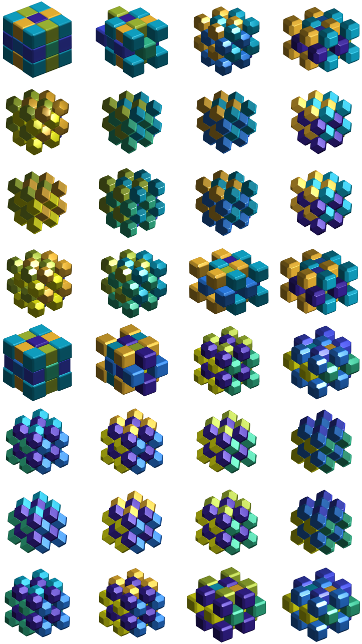

Consistency of Dirichlet partitions
— joint work with Todd Reeb (U. Utah)

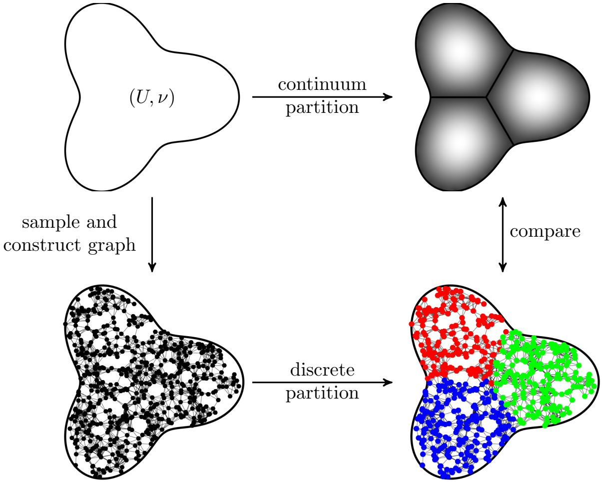

FIGURE 1. Illustration of consistency for the partitioning problem.

- Uses the $TL^2(\Omega)$ framework developed by N. Garcia Trillos and D. Slepčev.

Image processing and inverse problems — joint work with Dong Wang (U. Utah)

For $\tau > 0$, $\lambda \in (0,1)$, and a target-valued image, $f \in L^\infty(\Omega; T)$

$$\min_{u \in L^2(\Omega;T)} \ E_{\lambda,\tau}(u),$$

where

$$E_{\lambda,\tau}(u) = -\frac{1}{2}\langle u, (e^{\Delta\tau} - Iu\rangle \ + \ \frac{\lambda}{2}\langle u - f, e^{\Delta\tau}(u-f)\rangle.$$

Algorithm 1: A diffusion generated method for approximating minimizers of the energy in (2).

Input: Let $\tau, \lambda > 0$. Set $\Omega \in \mathcal{R}^d$, the target space as $T \in \mathcal{R}^k$, the image as $f \in H^1(\Omega, T)$ and the initial guess as $u_0 \in H^1(\Omega, T)$.

Output: A matrix-valued function $u_n \in H^1(\Omega, T)$ that approximately minimizes (2).

Set $s = 1$

while *not converged* **do**

  1. Diffusion Step. Solve the initial value problem for the diffusion equation until time τ with initial value given by $u_{s-1}(x)$:

$$\partial_t u(t,x) = \Delta u(t,x)$$
$$u(0,x) = \lambda u_{s-1}(x) + (1-\lambda) f.$$

  Let $\tilde{u}(x) = u(\tau, x)$

  2. Projection Step. Project $\tilde{u}(x)$ to T,

$$u_s = \Pi_T \tilde{u}.$$

  Set $s = s + 1$

Stability and convergence results for:

- $T \subset \mathbb{R}^k$ is a closed convex set
- $T \subset \mathbb{R}^k$ is a closed subset of the unit sphere, $\mathbb{S}^{k-1}$, such that the closest-point mapping, Π_T, is defined almost everywhere

Example: $T = \mathbb{S}^2$ valued signal

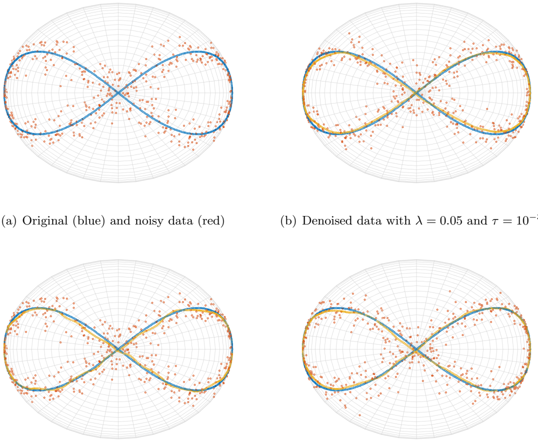

(a) Original (blue) and noisy data (red)

(b) Denoised data with $\lambda = 0.05$ and $\tau = 10^{-3}$

(c) Denoised data with $\lambda = 0.1$ and $\tau = 10^{-3}$

(d) Denoised data with $\lambda = 0.15$ and $\tau = 10^{-3}$

FIGURE 1. Results of the denoising an obstructed lemniscate of Bernoulli on the sphere, $\mathcal{S}^2$, with $\lambda = 0.05, 0.1$ and 0.15, respectively. In this simulation, τ is fixed as 10^{-3}. See Section 4.1.

compare to Bačák et al. A Second Order Nonsmooth Variational Model for Restoring Manifold-Valued Images. SISC (2016).

Example: Image of peppers in HSV space, $T = \mathbb{S}^1 \times \mathbb{R} \times \mathbb{R}$

Original image

Noisy image

$\lambda = 0.85$, $\tau = 10^{-4}$, PSNR$= 28.38$.

$\lambda = 0.9$, $\tau = 10^{-4}$, PSNR$= 28.41$.

Denoising the ”Peppers” image which is distorted with Gaussian noise on each of the red, green, and blue (RGB) channels with $\sigma = 0.1$ in hue, saturation, value (HSV) color space.

Example: Diffusion tensor MRI data, $T = \mathrm{SPD}(3)$

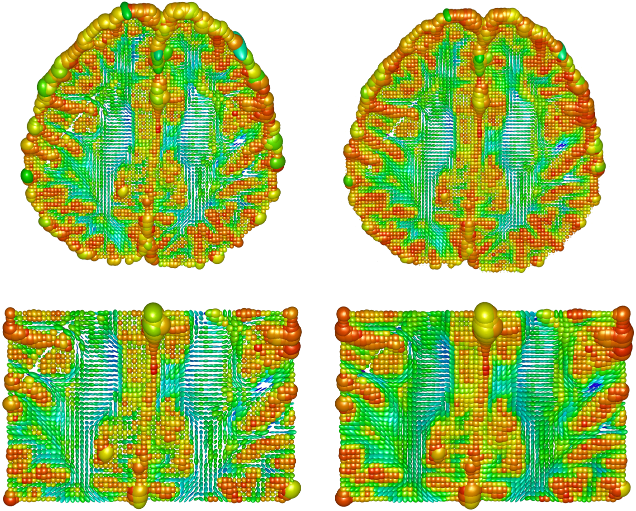

Denoising Camino DT-MRI data.
Left column: Slice 28 of the original data and a 'zoomed-in' subset.
Right column: Denoised data with $\lambda = 0.3$ and $\tau = 10^{-4}$ and the same subset.

Example: Fingerprint image, $T = \mathbb{RP}^1$

(a) Original fingerprint.

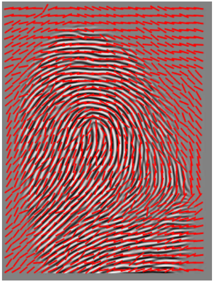

(b) Noisy orientation field on the fingerprint (a).

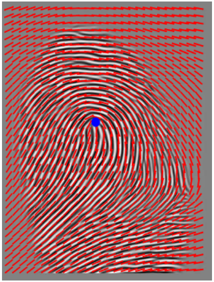

(c) $\tau = 10^{-2}$ and $\lambda = 0.15$.

(d) Original fingerprint.

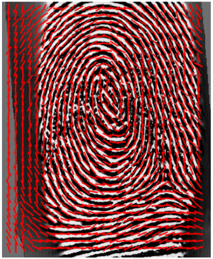

(e) Noisy orientation field on the fingerprint (d).

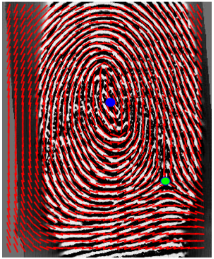

(f) $\tau = 10^{-2}$ and $\lambda = 0.15$.

Discussion and future directions for generalized MBO methods

- We considered a single matrix-valued field that has two "phases" given by when the determinant is positive or negative. It would be very interesting to extend this work to the multi-phase problem as was accomplished for $n = 1$ in [Esedoglu+Otto, 2015].
- For $O(n)$ valued fields with $n \geq 2$, the motion law for the interface is unknown.
- For the inverse problems considered, understand better the assumed noise model.
- Consider other image analysis tasks for target-valued maps: inpainting, segmentation, and registration

Thanks! Questions? Email: osting@math.utah.edu

B. Osting and D. Wang, Diffusion generated methods for denoising target-valued images, *submiteed, arXiv:1806.06956* (2018).

R. Viertel and B. Osting, An approach to quad meshing based on harmonic cross-valued maps and the Ginzburg-Landau theory, *submitted, arXiv:1708.02316* (2017).

B. Osting and D. Wang, A generalized MBO diffusion generated motion for orthogonal matrix valued fields, *submitted, arXiv:1711.01365* (2017).

D. Wang and B. Osting, A diffusion generated method for computing Dirichlet partitions, *submitted, arXiv:1802.02682* (2018).

B. Osting and T. H. Reeb, Consistency of Dirichlet Partitions, *SIAM J. Math. Analysis* (2017).

Y. van Gennip, N. Guillen, B. Osting, and A. Bertozzi, Mean curvature, threshold dynamics, and phase field theory on finite graphs, *Milan J. Mathematics* **82** (2014).

Thanks to support by NSF DMS 16-19755 and 17-52202.